2nd URSI AT-RASC, Gran Canaria, 28 May – 1 June 2018

Measurement of time-based arrays for massive tags localization

D. Masotti* (1) and A. Costanzo(2)
(1) DEI – University of Bologna, Bologna, Italy
(2) DEI – University of Bologna, Cesena, Italy

Abstract

The paper describes a time-based driving strategy of a compact antenna array suitable for future 5G IoT applications. Array elements are selectively activated in real-time for agile localization of and energy transfer to tagged objects, randomly distributed in harsh electromagnetic environments. The exploitation of time-modulation technique allows to simultaneously radiate at both the carrier frequency and the sideband harmonics due to the superposition of the nonlinear switches driving (or modulation) frequency. These arrays result in a very simple architecture if compared to standard arrays. Despite this, their characterization is not straightforward: in this paper some preliminary measurements of a two-element array for localization purposes are presented.

1. Introduction

The use of time-modulation has been successfully exploited for the realization of the so-called four-dimensional (4-D) arrays, where the time represents the additional dimension to be deployed in the realization of real-time reconfigurable radiating systems [1]. The idea of time-modulated arrays (TMAs) is extremely simple: each antenna port is controlled by a nonlinear switch, whose role is to activate/deactivate the corresponding radiating element through a periodic driving sequence. The duration of the ON/OFF period [2] and the ON instant [3] become additional optimization parameters, thus providing an almost infinite multi-dimensional design space in which the proper control sequence has to be chosen. The nonlinear radiating circuit regime is given by the superposition of the carrier radio-frequency (f_0) and the modulation frequency (f_M) used to periodically drive the switches. This paves the way to a radiation phenomenon of this array family, only: the capability to radiate power in correspondence of the sideband harmonics ($f_0 \pm hf_M$: h=1,2,…), too. The extreme simplicity of the TMA architecture, which avoids the use of complex phase shifters, makes these arrays very attractive for modern scenarios where sideband radiation can be fruitfully exploited: these applications range from direction finding [4], [5], and multi-harmonic radiation [6], to wireless powering [7], and cognitive radio [8] scenarios.

Despite their simplicity, TMAs need for an accurate and multi-domain design platform, consisting of the combination of Harmonic Balance-based circuit techniques and full-wave solvers [9]. Moreover, their laboratory characterization is not straightforward at all, because of the complex radiation mechanism and the delicate role of the nonlinear switches. In this paper, after a brief theoretical introduction to TMA behavior, some experimental data of a two-element TMA array are provided: the presented array can be exploited in localization of RF-ID tags in crowded and electromagnetically harsh environments, thanks to the multi-harmonic exploitation of the monopulse radar principle in conjunction with beam steering [10].

2. TMA radiation

Let us consider a linear array of N antennas operating at the carrier frequency f_0, with nonlinear switches at the antenna ports biased by periodic rectangular pulses $U_k(t)$, with period $T_M=1/f_M$ and duration τ_k (k = 1, 2, …, N). A schematic view of this simple architecture is shown in Fig. 1.

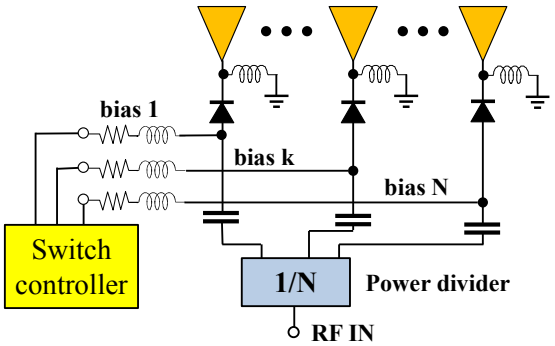

Figure 1. Scheme of a linear, N-element TMA, with diodes as switches, and bias networks.

The inclusion of time through the ON/OFF modulation of the switches in the excitation mechanism leads to a time-dependent array-factor definition:

$$AF(\psi,t)=\sum_{k=0}^{N-1}U_k(t)\,e^{jk\beta L\cos\psi}= \quad (1).$$
$$=\sum_{h=-\infty}^{\infty}e^{j2\pi(f_0+hf_M)t}\sum_{k=0}^{N-1}u_{hk}\,e^{jk\beta L\cos\psi}=\sum_{h=-\infty}^{\infty}AF_h(\psi)$$

where a uniform amplitude excitation condition is considered, L is the element spacing, β is the free-space phase constant, and ψ is the angle formed by the element alignment direction and the wireless link direction. The Fourier expansion of (1) (u_{kh} are the corresponding complex coefficients) provides harmonic components of the array-factor, which justify the sideband radiation phenomenon, i.e., the radiation at the carrier harmonics $f_0 \pm hf_M$, with h=0,1,2,…. The array synthesis procedure can thus make use of the additional complex coefficients of the Fourier expansion as design parameters:

$$u_{hk}=\frac{1}{T_M}\left(\frac{e^{-jh\omega_M t_{k,ON}}-e^{-jh\omega_M (t_{k,ON}+\tau_k)}}{jh\omega_M}\right) \quad (2).$$

where $t_{k,ON}$ is the ON instant of the $U_k(t)$ rectangular pulse. In this way, an almost infinite set of control sequences is available, and plenty of multi-harmonic radiation patterns can be synthesized.

3. TMA for localization

As example of application, let us consider a two-element array of planar monopoles on a layer of Taconic RF60A (ε_r=6.15, thickness=0.635 mm) operating at 2.45 GHz (see Fig. 2), properly fed through the bias sequence shown in Fig. 3 [4], where d represents a tuning parameter for varying the pulse duty-cycle. The two switches are two Schottky diodes, in particular the Skyworks SMS7630-079, largely used as rectifiers in energy harvesting applications because of their low threshold voltage: in the present case, they are periodically driven with the sequences of Fig. 2, with period T_M= 40μs, i.e., with modulation frequency f_M = 25 kHz.

The sideband radiation phenomenon can be favorably exploited in this case: in correspondence of the carrier f_0=2.45 GHz the two elements are excited in phase (because of the real nature of the corresponding Fourier coefficient u_{0k}), thus providing the standard Sum (Σ) radiation pattern; simultaneously, in correspondence of the first harmonics (h=±1), where the two dipoles, still in resonant condition, are out-of-phase because of the driving sequence of Fig. 2, a Difference (Δ) radiation pattern takes place. The further TMA capability consists in the tuning of the Δ pattern through the duty-cycle parameter d, whereas the Σ pattern is fixed (because of the real nature of the corresponding Fourier coefficient u_{0k}). Fig. 4 shows the result of a first simulation carried out by following the procedure described in [9]. The scanning plane is the xz-plane (see the reference frame of Fig. 3), hence the scanning angle is the elevation (θ).

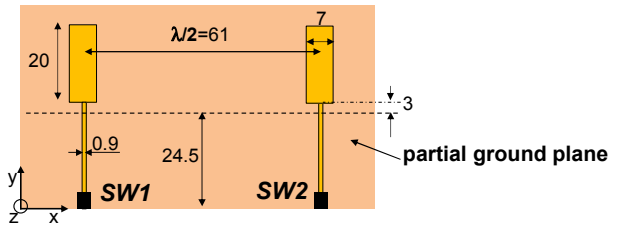

Figure 2. Two-monopole TMA on Taconic RF-60A (dimension in mm).

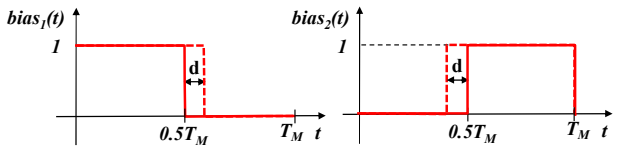

Figure 3. Excitation pulses waveforms, suitable for localization purposes.

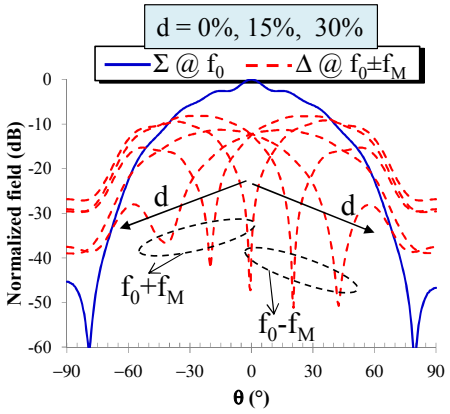

Figure 4. Simulated Σ and Δ radiation patterns, showing the tuning capability of the Difference by acting on parameter d.

In the localization of crowded RF-ID tags, radiation patterns as those of Fig. 4 can be extremely useful. By considering the backscattered Received Signal Strength Indicator (RSSI) from each illuminated tag, received both by the Σ and the Δ patterns of the TMA, the Maximum Power Ratio (MPR) figure of merit can be built, according to the following simple formula:

$$MPR(\theta)=\Sigma_{RSSI}^{dB}(\theta)-\Delta_{RSSI}^{dB}(\theta) \quad (3).$$

The sharp shape of the Δ steerable negative peaks is transferred onto the sharp positive peaks of the MPR patterns, as reported in Fig. 5. These patterns are able to guarantee high precision in the detection of both fixed [10] and moving tags [11]: a resolution up to few cm with a link distance of 3 m has been proven with a standard phased-array operating at 2.45 GHz [10].

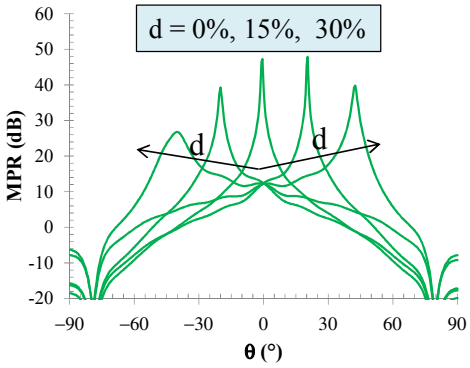

Figure 5. Simulated MPR patterns, showing their tuning capability by acting on parameter d.

4. Measurements

The TMA under exam has been realized with the Skyworks SMS7630-079 as switches. Fig 6 shows the corresponding prototype.

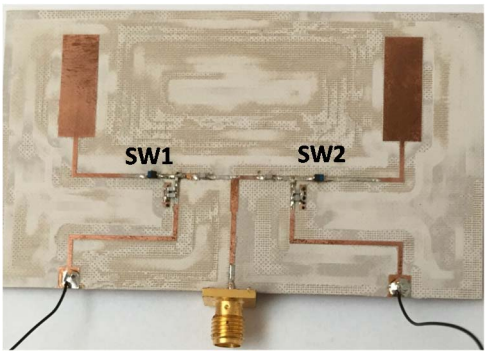

Figure 6. Photo of the two-monopole TMA prototype.

A microprocessor TI MSP430 is used to drive the diodes with waveforms of the kind of Fig. 3. As a first test, the TMA of Fig. 6 is connected to a signal generator providing the 2.45 GHz signal, and is placed in front of a TDK horn antenna connected to an RF spectrum analyzer: Fig. 7 reports the received spectra when the link direction θ is 0°, 30°, and 45° and the tuning parameter d assumes the 0% and 30% values. It is clearly visible the sideband radiation phenomenon (limited to the first lateral harmonics $f_0 \pm f_M$ in the figure), but also its dependency on both the link direction and the pulse duty-cycle: in fact the signal received by the Δ pattern at $f_0 \pm f_M$ increases with increasing values of θ if the biasing signals have duty-cycle=50% (d=0%), whereas it decreases if the duty-cycle is increased (d=30%), as confirmed by inspection of Fig. 4, too.

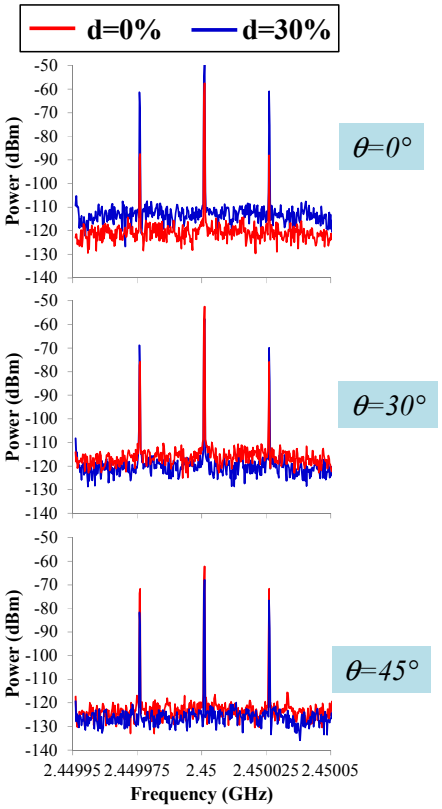

Figure 7. Measured multi-harmonic spectra for different θ directions and d values.

As a second test, the measurement of the Σ and Δ radiation patterns for d=0%, 30% is carried out. The results are shown in Fig. 8 and they reveal a good agreement with the predictions. However, there are some differences in terms of both the Δ minima position (error around 10°) and, most of all, the Δ field intensity. The reasons for this can be different: first of all the measurements are carried out in a real office scenario; secondly, the in house realization of the prototype can be responsible for slight asymmetries in the antennas feeding networks, thus causing a phase unbalance at the array ports; lastly, the switch model adopted in the simulation can be not extremely accurate as regards the diode package description: we experimentally verified that there is an undesired RF path through the capacitive parasitic of the Skyworks SMS7630-079. This unexpected current flow modifies the feeding mechanism, thus perturbing the delicate sideband radiation phenomenon. This investigation additionally shows that, for the exploitation of the huge potentialities of TMAs, the proper switch selection plays a crucial role.

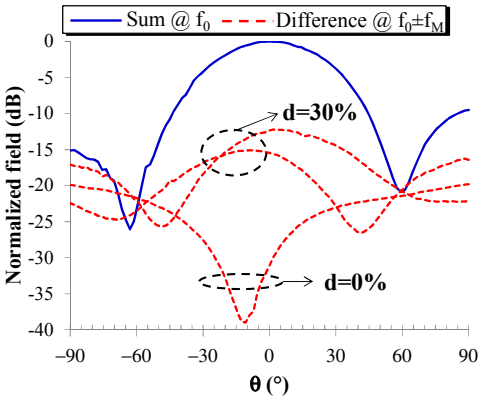

Figure 8. Measured multi-harmonic Σ and Δ radiation patterns for d=0% and 30%.

7. References

1. H. E. Shanks and R. W. Bickmore, “Four dimensional electromagnetic radiators," *Canadian J.l of Physics*, **37**, 3, 1959, pp. 263-275, doi: 10.1139/p59-031.

2. W. H. Kummer, A. T. Villeneuve, T. S. Fong, F. G. Terrio, “Ultra-low sidelobes from time-modulated arrays," *IEEE Trans. Antennas Propagat.*, **AP-11**, 6, Nov. 1963, pp. 633-639, doi: 10.1109/TAP.1963.1138102.

3. L. Poli, P. Rocca, L. Manica, and A. Massa, “Pattern synthesis in time-modulated linear arrays through pulse shifting," *IET Microwaves, Antennas & Propagation*, **4**,. 9, Sept. 2010, pp. 1157-1164, doi: 10.1049/iet-map.2009.0042.

4. A. Tennant e B. Chambers, “A Two-Element Time-Modulated Array With Direction-Finding Properties", *IEEE Ant. and Wirel. Prop. Lett.*, **6**, 2007, pp. 64-65, doi: 10.1109/LAWP.2007.891953.

5. D. Masotti, "A Novel Time-Based Beamforming Strategy for Enhanced Localization Capability," *IEEE Ant. and Wirel. Prop. Lett.*, **16**, 2017, pp. 2428-2431, doi: 10.1109/LAWP.2017.2722872.

6. L. Poli, P. Rocca, G. Oliveri, and A. Massa, “Harmonic beamforming in time-modulated linear arrays through particle swarm optimization," *IEEE Trans. on Ant. and Prop.*, **59**, 7, July 2011, pp. 2538-2545, doi: 10.1109/TAP.2011.2152323.

7. D. Masotti, A. Costanzo, M. Del Prete and V. Rizzoli, "Time-Modulation of Linear Arrays for Real-Time Reconfigurable Wireless Power Transmission," *IEEE Trans. Microw. Theory Techn.*, **64**, 2, Feb. 2016, pp. 331-342, doi: 10.1109/TMTT.2015.2512275.

8. P. Rocca, Q. Zhu, E.T. Bekele, S. Yang, A. Massa, "4-D Arrays as Enabling Technology for Cognitive Radio Systems," *IEEE Trans. Antennas Propag.*, **62**, 3, March 2014, pp.1102-1116, doi: 10.1109/TAP.2013.2288109.

9. D. Masotti, P. Francia, A. Costanzo, V. Rizzoli, "Rigorous Electromagnetic/Circuit-Level Analysis of Time-Modulated Linear Arrays," *IEEE Trans. Antennas Propag.*, 61, 11, Nov. 2013, pp.5465-5474, doi: 10.1109/TAP.2013.2279217.

10. M. Del Prete, D. Masotti, N. Arbizzani, A. Costanzo, "Remotely Identify and Detect by a Compact Reader With Mono-Pulse Scanning Capabilities," *IEEE Trans. Microw. Theory Techn.*, **61**, 1, Jan. 2013, pp.641-650, doi: 10.1109/TMTT.2012.2229290.

11. G. Paolini, M. Del Prete, F. Berra, D. Masotti and A. Costanzo, "An agile and accurate microwave system for tracking elderly people occupancy at home," *2016 IEEE MTT-S Latin America Microwave Conference (LAMC)*, 2016, pp. 1-3.